Numerical Methods in Civil Engineering

A simple and efficient plasticity-fracture constitutive model for confined concrete

Hadi Meidani *

ARTICLE INFO

Article history:
Received:
May 2014.
Revised:
September 2014.
Accepted:
January 2015.

Keywords:
Plasticity-fracture,
Constitutive model,
Confined concrete

Abstract:

A plasticity-fracture constitutive model is presented for prediction of the behavior of confined plain concrete. A three-parameter yield surface is used to define the elastic limit. Volumetric plastic strain is defined as hardening parameter, which together with a nonlinear plastic potential forms a non-associated flow rule. The use of non-associated flow rule improves the prediction of the dilation behavior of concrete under compressive loading. To model the softening behavior, a fracture energy-based function is used to describe strength degradation in post-peak regime. The Euler-forward algorithm is used to integrate the constitutive equations. The proposed model is validated against the results of triaxial compressive experiments. Finally, the behavior of plain concrete confined by layers of carbon fiber reinforced polymer is studied to show capability of the model for passive confinement.

1. Introduction

In recent years, the emphasis on cost-efficient use of concrete as a structural material has resulted in an increasing attention towards the nonlinear analysis of concrete structures. This trend is all the more important when the efforts in improving computational techniques are combined with the ever increasing capabilities of digital computers. These techniques can ensure structural safety and cost-efficiency by taking advantage of the nonlinear behavior of concrete.

Complex nonlinearities of plain concrete stem from its nonlinear stress-strain behavior, tensile cracking, crushing failure and creep-induced strains. All these characteristics strongly depend on triaxial states of stress. In a nonlinear analysis, aside from the numerical method used to solve the equations, the way the material behavior is modeled plays a significant role in the validity of the analysis. Therefore,it is necessary to concentrate serious efforts on correct description of material behavior and its implementation in a numerical algorithm.

**Corresponding Author: Assistant Professor, Department of Civil and Environmental Engineering at the University of Illinois at Urbana ,USA . Email : meidani@illinois.edu*

Various investigations have focused on proposing a proper description of concrete behavior under triaxial compression. Among the proposed models, only a few describe the entire response spectrum based on a unified formulation. In such cases, a constitutive model capable of describing various behaviors of concrete using unified formulation would invariably decrease the computational efforts.

Considering the significant inelastic compressive behavior of concrete, the theory of plasticity is regarded as the most efficient basis to formulate the compressive behavior of concrete. Recent researches on plasticity-based constitutive modeling include a model by Imran and Pantazopoulou [1] in which damage is quantified by the volumetric expansion together with a non-associated flow rule. The softening behavior is modeled based on a formulation other than fracture energy base. Also in the literature is the model proposed by Grassl et al. [2] which uses volumetric plastic strain as the hardening parameter which together with a nonlinear non-associated flow rule constitutes the hardening formulation. The softening model is based on axial behavior of two specimens under different levels of confinement. More recently, Shen *et al.* [3] has proposed a constitutive model based on Drucker-Prager-type plasticity.

To increase the compressive strength of concrete materials, the elements under compression are wrapped by Fiber Reinforced Polymer (FRP) layers resulting in different behavior for the confined material. Among the recent researches on constitutive modeling for FRP-confined concrete, Spoelstra and Monti [4] have proposed a uniaxial model which is suitable for fiber type modeling, in which the cross section of the element is divided into a number of fiber elements with specified uniaxial stress strain relation.

To take into account the effects of lateral confining stress on the axial performance of concrete, Mirmiran and Shahawy [5] investigated the difference between the behaviors of steel- and FRP-confined concrete. They performed several experiments on concrete columns and concluded that the dilation behavior of concrete leads to difference between the behaviors of steel- and FRP-confined concrete. Later, Samaan *et al.* [6] proposed a bilinear stress-strain relation for the behavior of concrete in axial and lateral direction. Xia and Wu [7] have also proposed a bilinear relation between the stress and strain of FRP-confined concrete in axial and lateral directions and performed several experiments to verify the model.

The current paper describes and summarizes the formulation of a plasticity-fracture constitutive model for confined concrete. As discussed before, the theory of plasticity is regarded as a suitable basis for modeling the hardening behavior of concrete. In comparison with the other constitutive models, the current model uses volumetric plastic strain as the hardening parameter. This parameter enables the model to correctly include the dilation characteristics of concrete. For softening branch, different from the aforementioned recent models, the current model uses fracture energy method. Since the failure characteristics of concrete are governed by the development of cracks, the fracture energy becomes a more reasonable choice.

The simple triaxial formulations of the current model have enabled it to be used widely in analysis program. It will be shown that the behavior of FRP-confined concrete is well predicted by this model, while it has not the shortcomings of an axial or biaxial stress-strain relations proposed for this kind of modeling (Spoelstra and Monti [4], Mirmiran and Shahawy [5], Samaan *et al.* [6] and Xia and Wu [7]).

2- Hardening Behavior

Concrete is a semi-brittle heterogeneous material consisted of aggregates, air voids, water and cement. Nevertheless, for simplicity, an isotropic behavior is often assumed for plain concrete. This assumption does not significantly sacrifice the accuracy. To model post-yield behavior of concrete in the hardening branch, plasticity formulation is used. In plasticity formulation there should exists a yield surface, a hardening law and a flow rule. The yield surface defines elastic limit. The hardening law describes the evolution of loading surface. The flow rule defines the plastic strain vector.

In general, numerical integration of constitutive equations is accomplished by predicting an elastic behavior which results in an elastic predictor stress. During each increment, if plastic loading occurs, the elastic predictor stress is returned to a suitably updated yield surface ensuring that consistency condition is maintained. Over the last three decades, many algorithms for constitutive integration of various elastoplastic models have been developed. Of these algorithms, the Euler forward algorithm has remained the most popular due to its simplicity and its avoidance of large iterations at Gauss-point levels.

In current constitutive modeling, an Euler forward algorithm is used to integrate the rate-independent, small-deformation elastoplastic formulations. The elastoplastic tangent modulus, as described later, is constituted, using Euler forward algorithm, as

$$D_{ijkl}^{ep} = D_{ijkl} - \frac{1}{H}\frac{\partial \mathrm{f}}{\partial \sigma_{\mathrm{mn}}} \mathrm{D}_{\mathrm{mnkl}}\, D_{ijpq}\frac{\partial g}{\partial \sigma_{pq}} \tag{1}$$

Where D_{ijkl} is the elastic modulus, f is the yield surface, g is the plastic potential and H is defined by

$$H = \frac{\partial f}{\partial \sigma_{ij}}\; D_{\mathrm{ijkl}}\frac{\partial g}{\partial \sigma_{kl}} - \frac{\partial f}{\partial q}.\frac{\mathrm{dq}}{\mathrm{d}\kappa}.\delta_{ij}\frac{\partial \mathrm{g}}{\partial \sigma_{\mathrm{ij}}} \tag{2}$$

where q is the hardening function and κ is the hardening parameter.

In each load increment, first an elastic predictor stress is calculated. If the stress lies outside the yield surface, it is corrected by consistency condition and the elastoplastic modulus is used to evaluate the stress increment from the strain increment.

The yield surface used in this paper is a three-parameter criterion proposed by Menetrey and Willam [8]. The criterion is formulated in the Haigh-Westergard space, as

$$f = \left(\sqrt{1.5}.\rho\right)^2 + q_h(\kappa).m.\left[\frac{\rho}{\sqrt{6}}.r(\theta,e) + \frac{\xi}{\sqrt{3}}\right] - q_h(\kappa)\,q_s(\kappa) \le 0 \tag{3}$$

Where ρ is the deviatoric stress, ξ is the hydrostatic pressure, q_h and q_s are hardening and softening functions, respectively, and θ and e are two parameters for defining the yield surface which will be explained later. The parameters *m* and *r* are defined by equations (4) and (5):

$$m = 3.\frac{f_c^{\,2} - f_t^{\,2}}{f_c.f_t}.\frac{e}{e+1} \tag{4}$$

where f_c and f_t are the compressive and tensile strength of concrete,

$$r(\theta, e) = \frac{4(1-e^2).\cos^2\theta + (2e-1)^2}{2(1-e^2).\cos\theta + (2e-1).\left[4(1-e^2).\cos^2\theta + 5e^2 - 4e\right]^{\frac{1}{2}}} \quad (5)$$

This failure criterion is a combination of the maximum tensile stress condition of Rankine (cut-off condition) and the Mohr-Coulomb friction law of limited shear strength. It provides a fair description of tensile/cohesive strength of cementitious materials as well as a reasonable description of shear strength of frictional materials. It takes into account the effect of all three principal stresses. Besides, the friction and cohesion parameters are decoupled so that direct control on hardening and softening behavior would be possible. The eccentricity *e* describes the out-of-roundness of the deviatoric trace of yield surface. It is recommended to set $0.5 \le e \le 0.6$ to predict an acceptable equi-biaxial strength envelope for low and medium strength concretes (Menetrey and Willam [8])

In this constitutive modeling, the volumetric plastic strain is used as hardening parameter, which is defined as

$$\dot{\kappa}\left(\dot{\varepsilon}_{ij}^{p}\right) = \dot{\varepsilon}_{v}^{p} = \delta_{ij}\,\dot{\varepsilon}_{ij}^{p} \quad (6)$$

This parameter depends on hydrostatic pressure, and can consequently include the effects of this pressure on concrete behavior. Therefore, no other function is required to be calibrated, and fewer parameters are included in the formulation.

The aforementioned hardening parameter together with a nonlinear plastic potential defines the hardening behavior of concrete (Grassl *et al.* [2]). As mentioned, the plastic flow defines the plastic strain with the aid of a function, *g*, called plastic potential. Here a non-associated flow rule is used, i.e., the plastic potential is different from the yield surface. Since approximating the plastic potential with a quadratic function result in good agreement with experimental data, the nonlinear plastic potential is defined as (Grassl *et al.* [2]):

$$g = -A.\rho^2 - B.\rho + \xi = 0 \quad (7)$$

Two parameters of plastic potential need to be calibrated based on uniaxial and triaxial compression test data. As mentioned before, the volumetric plastic strain is chosen as the hardening parameter. There are three fundamental assumptions based on which the two parameters are calibrated, as follows (Grassl et al. [2]):

a. The peak stress in uniaxial compression f_c, corresponds to zero volumetric strain. This assumption is corroborated by reports by Kupfer *et al.* [9], Van- Mier [10], and Imran [11].

b. The failure threshold for all stress states is assumed to be volumetric plastic strain in peak stress in uniaxial compression.

c. The inclination of total plastic strain is equal to the inclination of plastic strain increment at corresponding stress state. The report by Smith [12] supports this assumption.

Therefore, parameters *A* and *B* are derived as below

a. Plastic strain at the peak stress in uniaxial compression

The axial component of plastic strain is equal to the total axial strain minus the elastic portion:

$$\varepsilon_{33}^{p} = \varepsilon_{33} - \left(-\frac{f_c}{E}\right) \quad (8)$$

and considering zero volumetric strain at the peak stress, the lateral components are derived as

$$\varepsilon_{11}^{p} = \varepsilon_{22}^{p} = -\frac{1}{2}\varepsilon_{33} - \upsilon\frac{f_c}{E} \quad (9)$$

Therefore, the volumetric plastic strain would be equal to the volumetric elastic strain, as

$$\varepsilon_{v}^{p} = \varepsilon_{11}^{p} + \varepsilon_{22}^{p} + \varepsilon_{33}^{p} = \frac{f_c}{E}.(1-2\upsilon) \quad (10)$$

b. Plastic strain at the peak stress state in triaxial compression

The axial component of plastic strain at peak stress state is therefore, as

$$\varepsilon_{33}^{p} = \varepsilon_{33} - \frac{1}{E}.\left(\sigma_{33} - \upsilon.(\sigma_{11} + \sigma_{22})\right) \quad (11)$$

and the lateral components are

$$\varepsilon_{11}^{p} = \varepsilon_{22}^{p} = \frac{\varepsilon_{v}^{p} - \varepsilon_{33}^{p}}{2} \quad (12)$$

Using Eqs. (8) to (12), the inclination of plastic strain at peak stress in uniaxial and triaxial compression states is calculated as

$$\tan\psi = \sqrt{\frac{2}{3}}\,\frac{\left(\varepsilon_{33}^{p} - \varepsilon_{11}^{p}\right)}{\varepsilon_{v}^{p}} \quad (13)$$

Besides, the length of deviatoric stress vector is derived for uniaxial compression as

$$\rho_1 = \sqrt{\frac{2}{3}} \quad (14)$$

and for triaxial compression, as

$$\rho_2 = \sqrt{\frac{2}{3}}.\frac{(\sigma_{11} - \sigma_{33})}{f_c} \quad (15)$$

The inclination of the total strain is derived by

$$\frac{\partial g(\rho,\xi)}{\partial \rho} = -2A\rho - B = \tan\psi \tag{16}$$

and finally, the two parameters A and B are determined by solving a set of two equations corresponding to two different stress states

$$A = \frac{(\tan\psi_2 - \tan\psi_1)}{2.(\rho_1 - \rho_2)} \tag{17}$$

$$B = \rho_1.\frac{(\tan\psi_1 - \tan\psi_2)}{(\rho_1 - \rho_2)} - \tan\psi_1 \tag{18}$$

where the indices indicate the corresponding stress state.

3. Strain-Softening Behavior

There are different methods for modeling strain-softening behavior of plain concrete. Among them, plasticity-based models and continuum damage mechanics are categorized in the continuum mechanics approach. Originally developed for metals, classic plasticity theory fails to present an acceptable description of failure process in concrete due to its fundamentally different nature. Therefore, some modified plasticity models have been proposed for plain concrete.

The plasticity-based and continuum damage-based models regard the strain-softening as a distributed or average characteristic. On the other hand, the crack band model (Bazant et al. [13]) and the fictitious crack model (Hillerborg et al. [14]) deal with localized tensile crack based on the concept of fracture energy. There are computational advantages in using a distributed fracture versus localized crack based models.

Among others, Pramono and Willam [15] have proposed a fracture energy-based macro model describing the loss of strength in post peak regime based on the loss of tensile strength with increasing crack displacement. The softening function is thus defined as a function of uniaxial tensile stress

$$q_s = \frac{\sigma_t}{f_t} \tag{19}$$

in which σ_t is defined as

$$\sigma_t = f_t \exp\left(-5\frac{u_f}{u_r}\right) \tag{20}$$

in which u_f is crack displacement and u_r is rupture displacement. The crack displacement is related to the fracture strain as

$$\dot{u}_f = \frac{G_f^I}{G_f^{II}}.\dot{\varepsilon}_f \tag{21}$$

and $\frac{G_f^I}{G_f^{II}}$ is proposed as a function of major principal stresses as

$$\frac{G_f^{II}}{G_f^I} = A_s\left(\frac{\sigma_1}{f_c} - \frac{f_t}{f_c}\right)^4 + B_s\left(\frac{\sigma_1}{f_c} - \frac{f_t}{f_c}\right)^2 + 1 \tag{22}$$

where σ_1 is the normal stress in which the parameters A_s and B_s are determined using test data with low and high levels of confinement.

The softening function used in present study is defined as a function of tensile crack displacement. It is calibrated by a function for taking into account the effects of different levels of confinement on post-peak behavior, as

$$q_s = \exp\left(\frac{\left(\frac{u_f}{u_r}\right)}{A_s.\xi^2 + B_s}\right) \tag{23}$$

The increment of tensile crack displacement is defined as

$$\dot{u}_f = h_t.\dot{\varepsilon}_f \tag{24}$$

in which h_t is crack spacing and $\dot{\boldsymbol{\varepsilon}}_f$ is defined as

$$\dot{\varepsilon}_f = \sqrt{\left\langle \dot{\varepsilon}_f \right\rangle^T \left\langle \dot{\varepsilon}_f \right\rangle} = \dot{\lambda}\left\|\left\langle \frac{\partial g}{\partial \sigma} \right\rangle\right\| \tag{25}$$

where <.> denotes the length of the vector. The two parameters in the softening function are calibrated using the data of two experiments with different confinement levels. The curves of the proposed models with different values of A_s and B_s are compared with corresponding test data until the parameters result in curves which are in reasonable agreement with the two data sets. The softening function is schematically illustrated in Fig. 1.

Finally, the remaining problem is to integrate the softening constitutive equations. Satisfying the consistency condition, the updated stress is related to the total strain through an elastoplastic modulus, as [16]

$$D_{ijkl}^{ep} = D_{ijkl} - \frac{\frac{\partial \mathrm{f}}{\partial \sigma_{\mathrm{mn}}} \mathrm{D}_{\mathrm{mnkl}}\, D_{ijpq} \frac{\partial g}{\partial \sigma_{pq}}}{\frac{\partial f}{\partial \sigma_{ij}}\, D_{\mathrm{ijkl}} \frac{\partial g}{\partial \sigma_{kl}} - \frac{\partial f}{\partial q_s} \cdot \frac{\partial q_s}{\partial u_f}.\dot{u}_f} \tag{26}$$

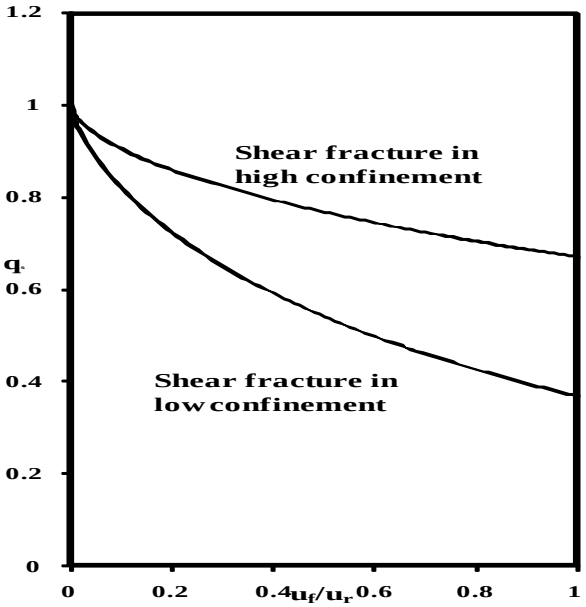

Fig.1: Schematic illustration of softening function

4. Verification

The capability of proposed model is evaluated in comparison with experimental data of confined concrete. The proposed constitutive equations are used in a computer program to produce stress-strain behavior of concrete based on the assumption that the confining stresses remain constant during loading, i.e., active confinement.

The performance of the proposed model is compared with the results of triaxial compression test by Imran [11] for different levels of confinement. The comparisons are presented in the stress-strain curves in the axial and lateral directions in Figs. 2 to 5. The model parameters are set to f'_c=47.4 MPa, f_t=4.74 MPa, E=30 GPa, □=0.15, and e=0.52. The hardening and softening functions are calibrated as A_h=-15.63, B_h=32.26, A_s=0.07, B_s=0.12.

The performance is also verified by comparison with the experimental data reported by Kotsovos and Newman [17]. The comparison is illustrated in Figs. 6 to 9. The concrete specimens are loaded under four different levels of confinement, i.e., 18 MPa, 35 MPa, 51 MPa, and 70 MPa. The material properties are set to E= 30 GPa, □ = 0.15, f_c = 46.9 MPa, f_t = 4.69 MPa, and e = 0.52.

The performance of the model under high hydrostatic pressures is also verified by comparison with the experimental data of Bazant et al. [18] in Figs. 10 to 12. The model parameters are set to E = 35 MPa, □ = 0.18, f'_c = 45.5 MPa, f_t = 4.55 MPa, and e = 0.52.

Good agreement observed in prediction of stress-strain relations of experiment results in both the medium and high levels of confinement pressure.

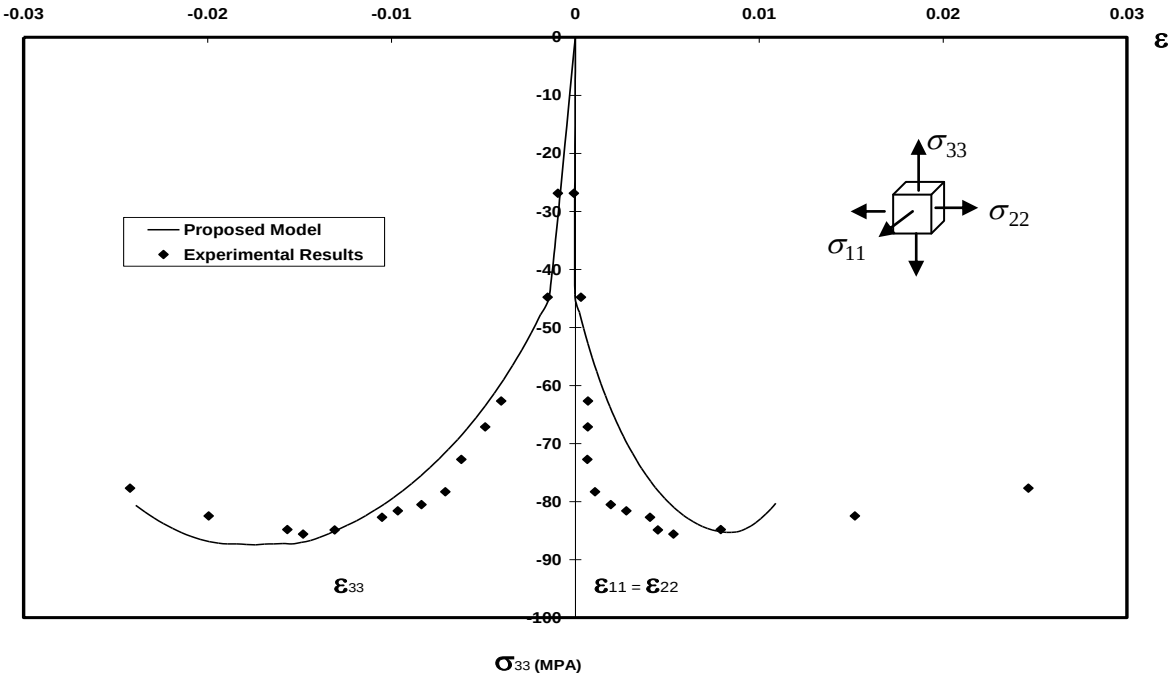

Fig.2: Comparison of the proposed model with results of 8.6 MPa confinement experiment

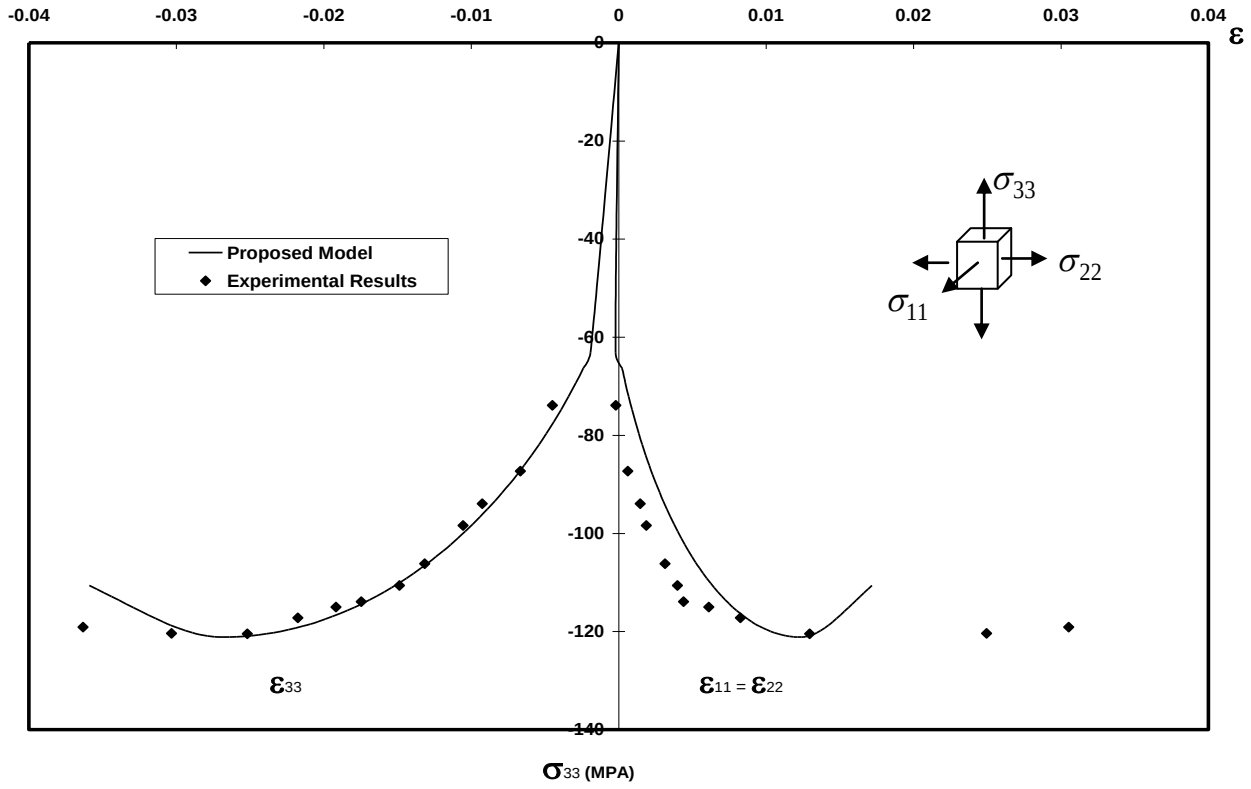

Fig.3: Comparison of the proposed model with results of 17.2 MPa confinement experiment

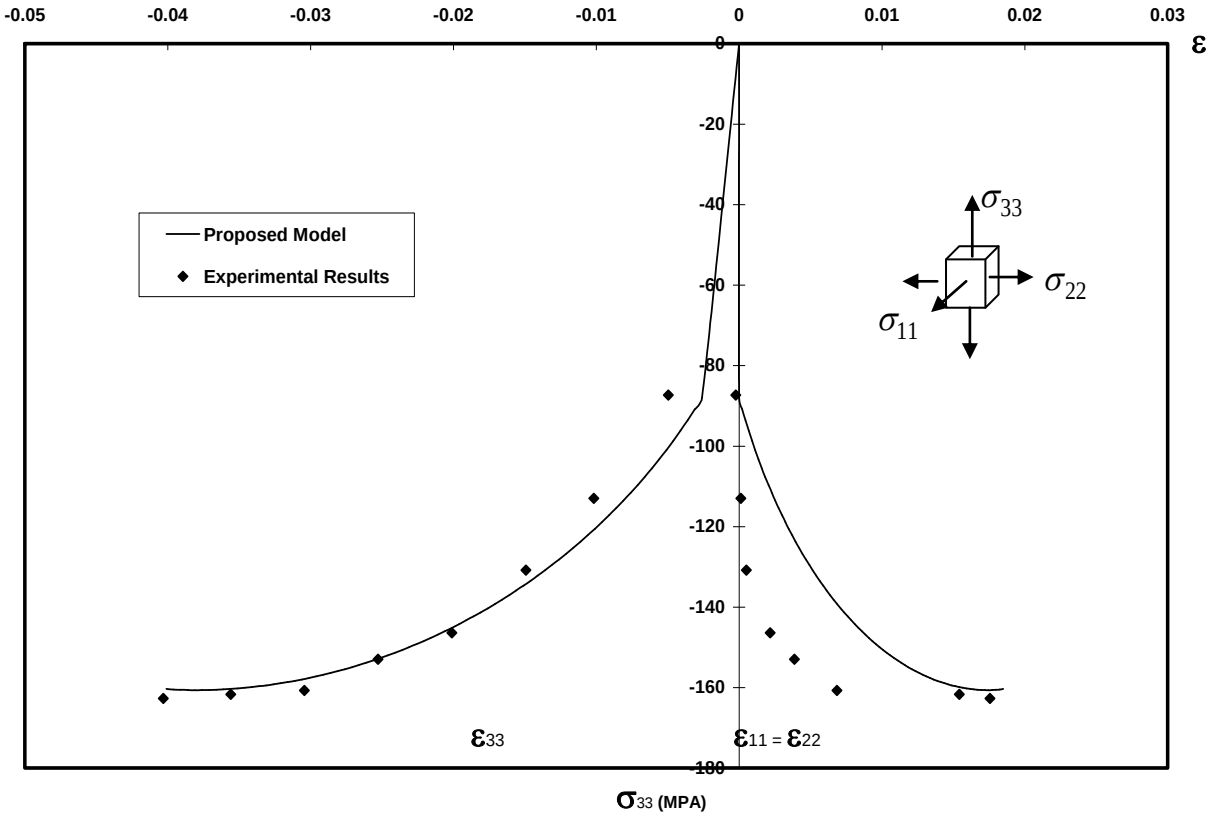

Fig.4: Comparison of the proposed model with results of 30.1 MPa confinement experiment

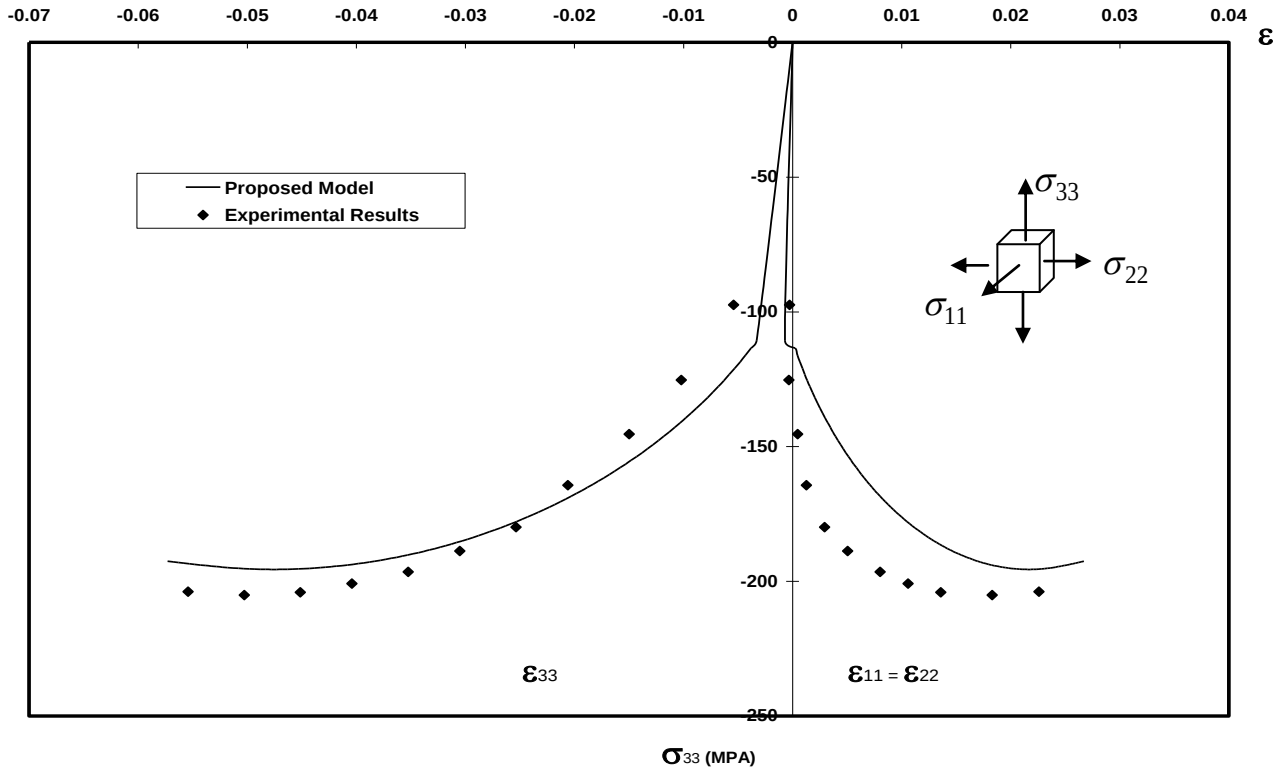

Fig.5: Comparison of the proposed model with results of 43 MPa confinement experiment

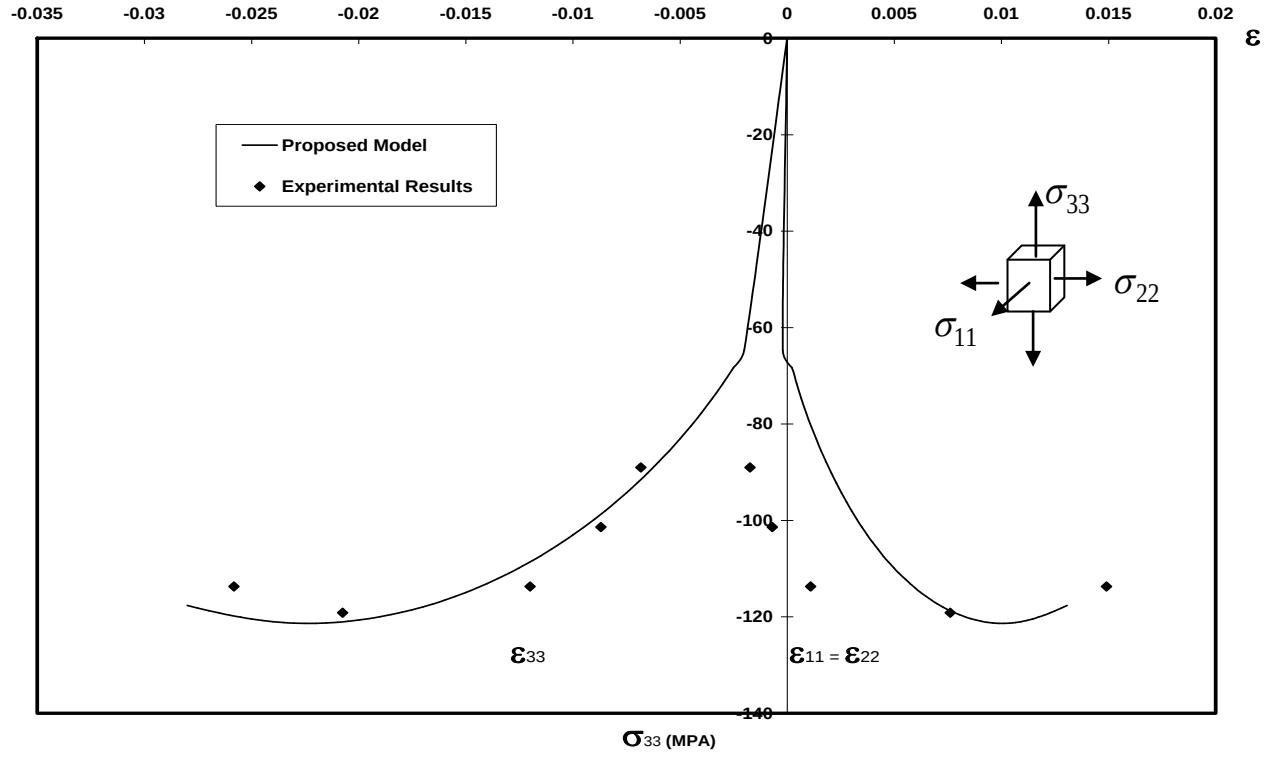

Fig.6: Comparison of the proposed model with results of 18 MPa confinement experiment

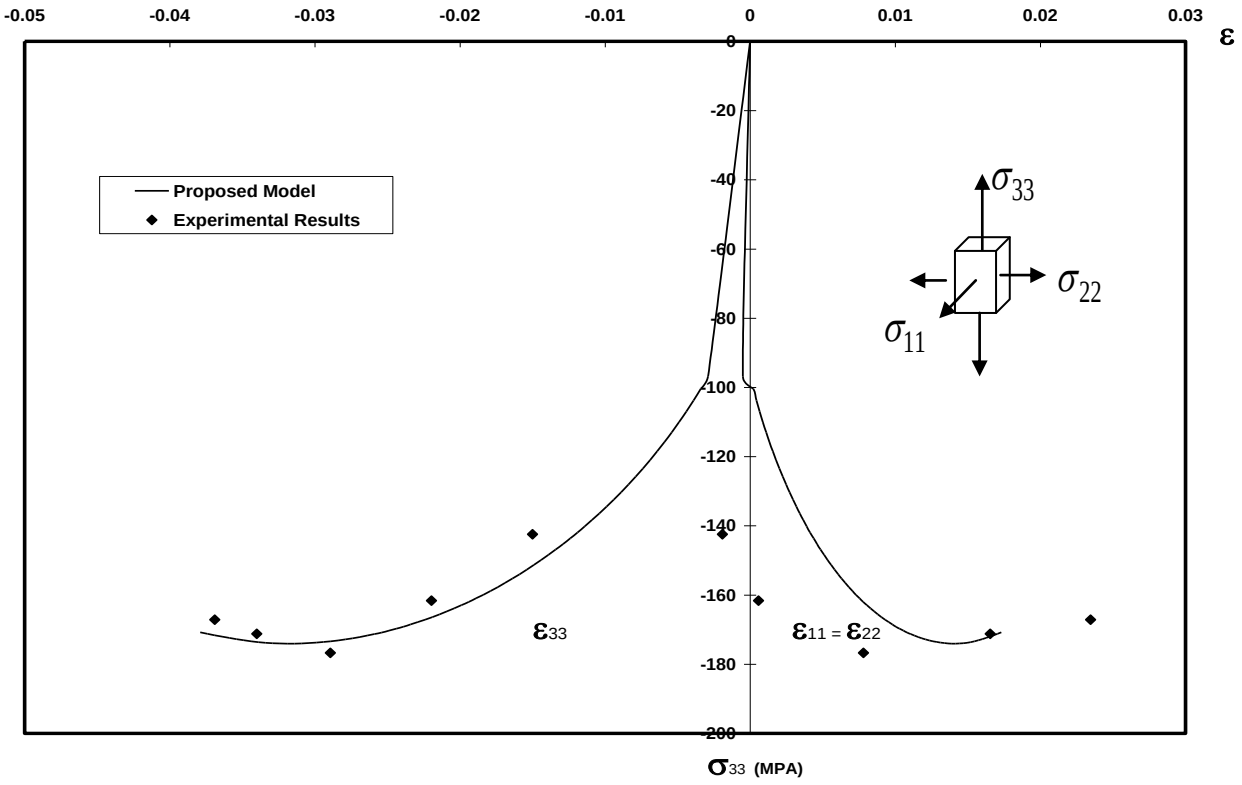

Fig.7: Comparison of the proposed model with results of 35 MPa confinement experiment

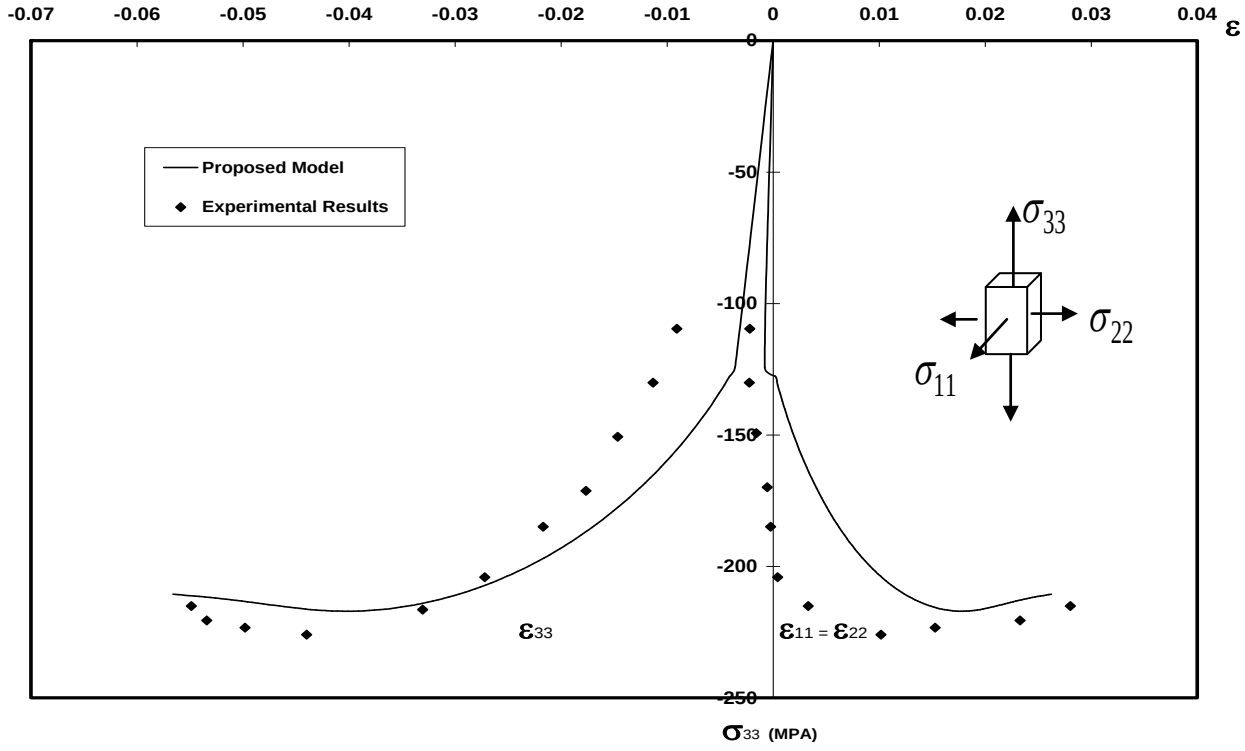

Fig.8: Comparison of the proposed model with results of 51 MPa confinement experiment

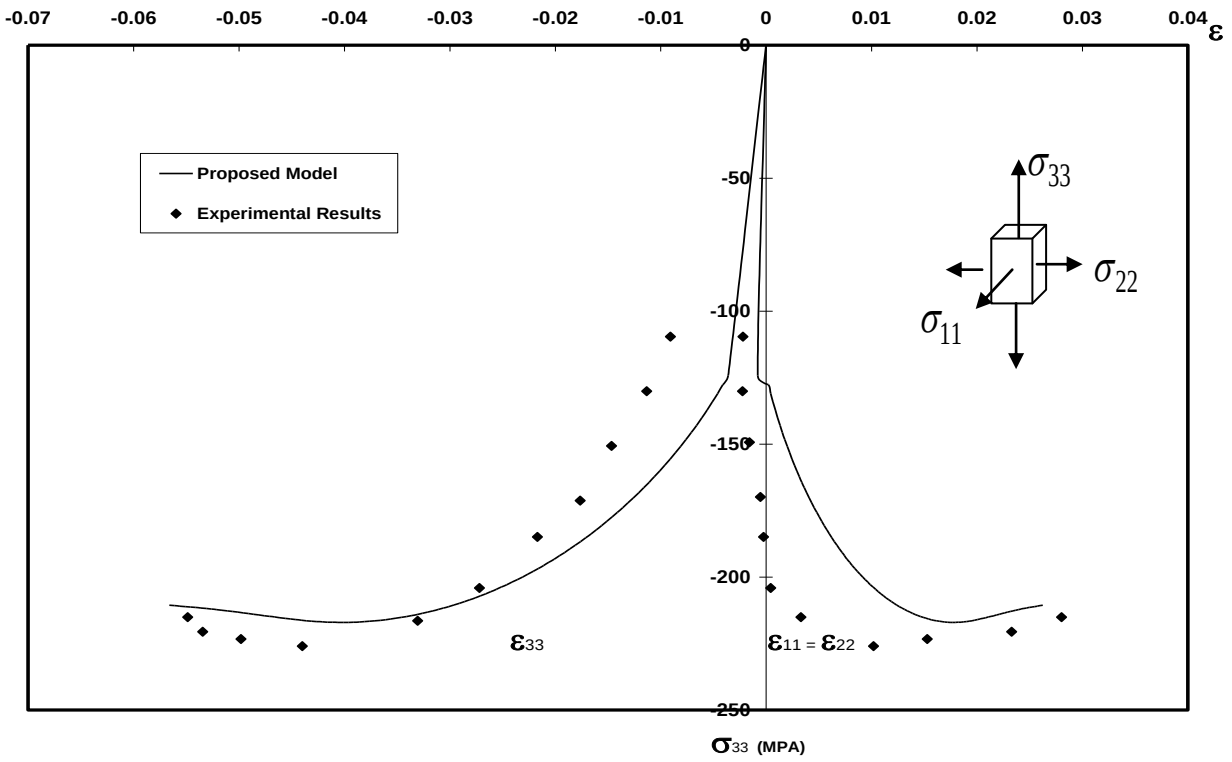

Fig.9: Comparison of the proposed model with results of 70 MPa confinement experiment

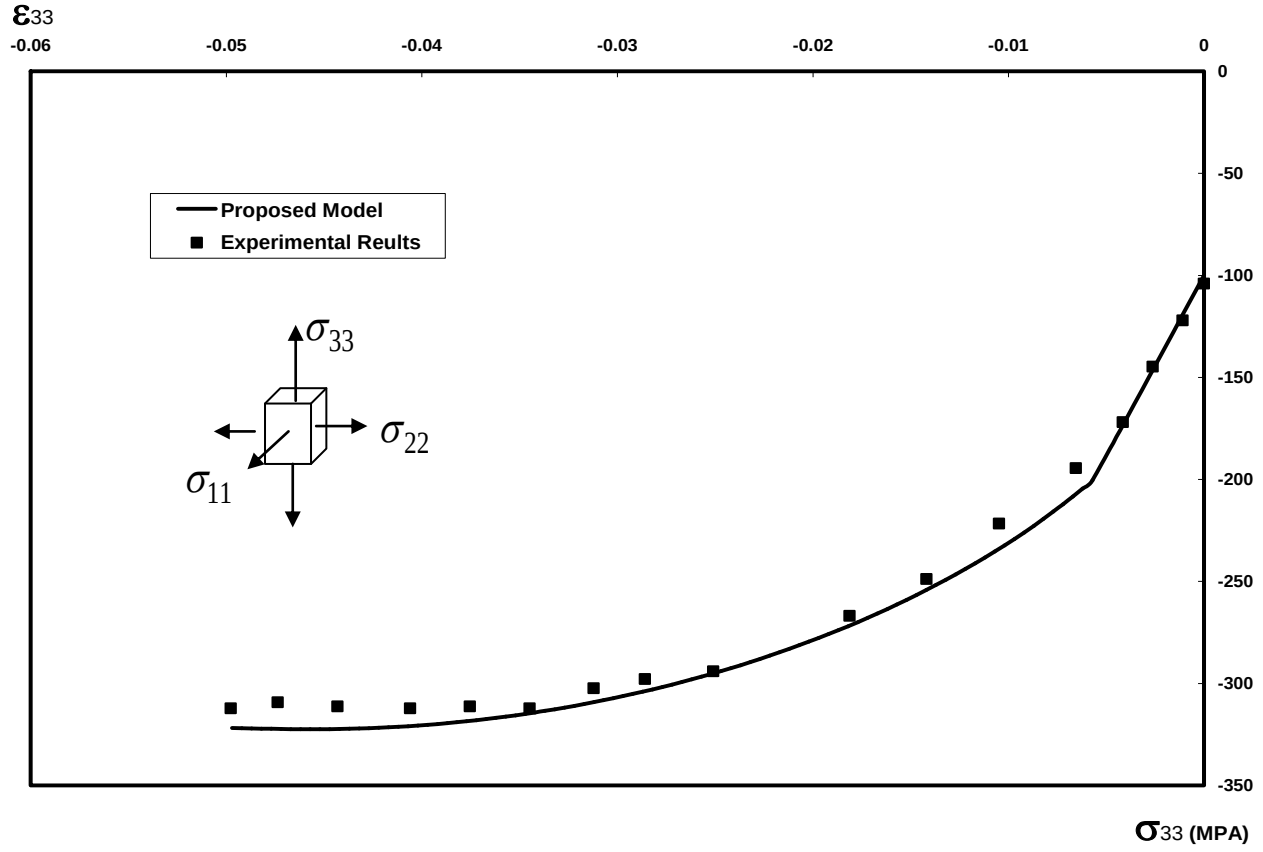

Fig.10: Comparison of the proposed model with results of 100 MPa confinement experiment

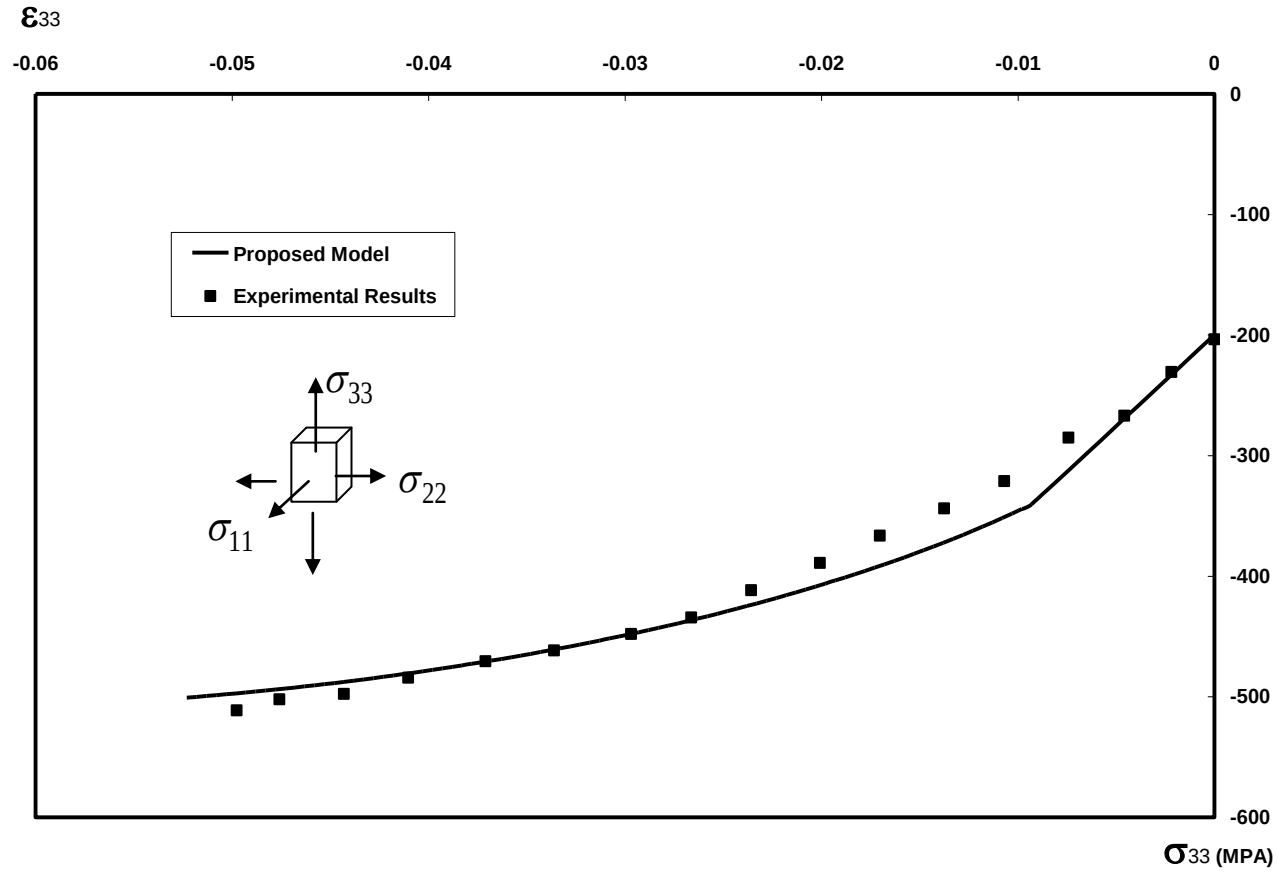

Fig.11: Comparison of the proposed model with results of 200 MPa confinement experiment

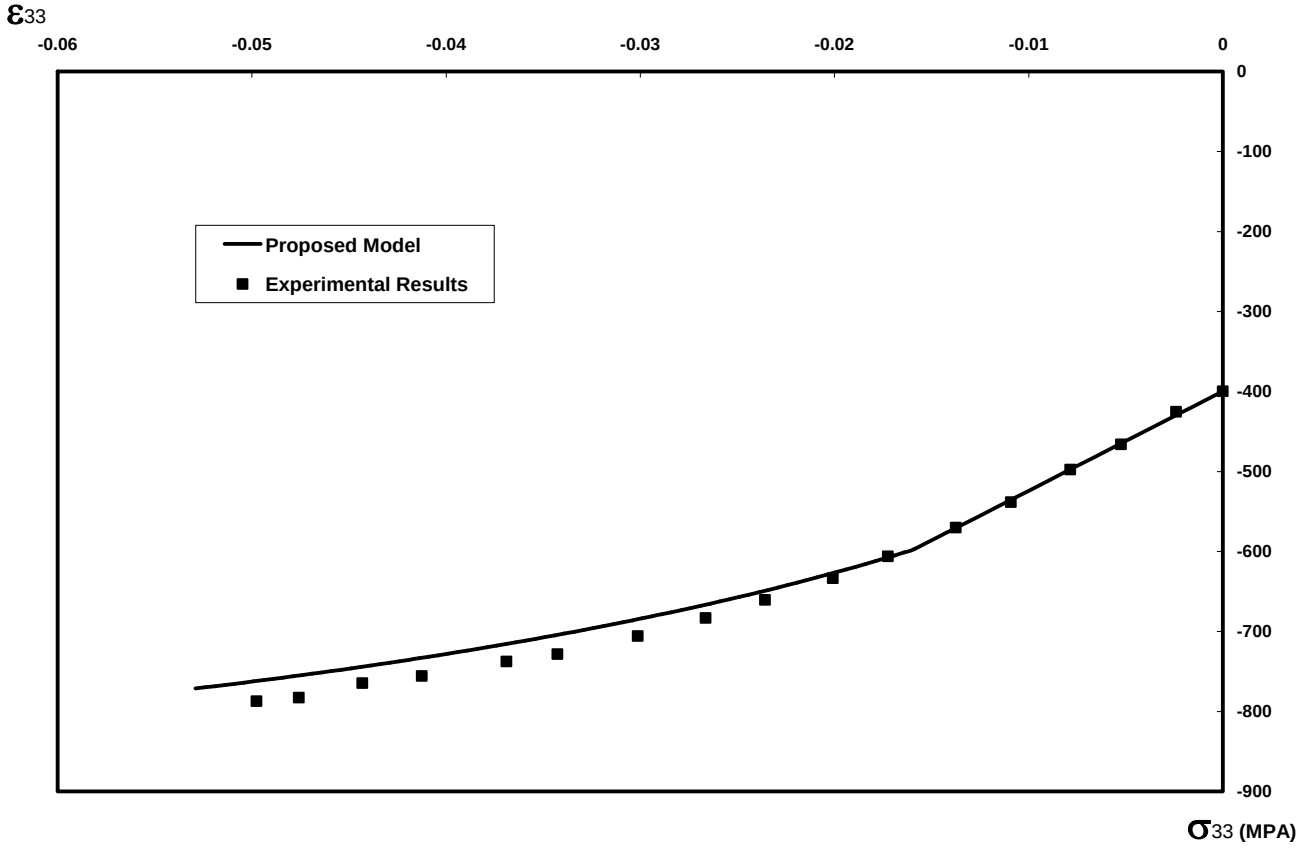

Fig.12: Comparison of the proposed model with results of 400 MPa confinement experiment

5. Passively Confined Plain Concrete

The objective of this section is to demonstrate the need of considering the different governing equations for passively confined concrete. As mentioned earlier, the confinement significantly affects strength and ductility of concrete. The confinement in structural concrete is activated by preventing its lateral dilation through circumferential restraining mechanisms. Therefore, the confining stresses depend on the strains imposed during the loading, hence accentuating the need of including passive confinement relationships.

The confining stresses in the model should account for the passive nature of the confinement mechanism, through the use of two springs in the two lateral directions which correlate the confining stresses to the lateral strains of concrete core.

In the present study, the behavior of plain concrete confined by carbon fiber reinforced polymer (CFRP) layers is considered. The confining layers remain linear elastic to failure, thus it is expected that up to final steps of loading, plain concrete undergoes increasing confinement.

The constitutive equations of passively confined plain concrete are studied by Grassl et al. [2]. Fig. 13 shows the free body diagrams, based on which the formulations are developed. Only the concrete core is assumed to be loaded. The cohesive stresses at the interface of concrete and CFRP layers are neglected, and the radial stresses are assumed to be constant and uniform throughout the cross section. Finally, the radial stiffness created by confining layers, K_r, is derived in term of the axial tensile stiffness of the layers, E, as

$$K_r = \frac{t}{r}.E. \qquad (27)$$

The element considered in the present study is a 3D element confined in the two lateral directions by linear springs and loaded in the axial direction (Fig. 14). The behavior of CFRP layers is assumed to remain elastic up to the ultimate stress. The Young modulus of the layers is set to E = 100 GPa and the ultimate stress is set to σ_u = 2000 MPa. A specimen with the radius r=75 mm confined by 1mm CFRP layers is analyzed. According to Eq. (27), the radial stiffness would be K_r = 1.33 GPa.

The results of the analysis performed considering passive confinement equations are presented in Fig. 15. The analysis is terminated when either the radial confining stresses reaches its ultimate value or the confined concrete reaches its failure. It can be inferred from the curve that the axial stress continually increases up to the failure of the specimen, mainly due to the increasing level of confining stresses in the CFRP jacket. This reinforces the earlier note that modeling of plain concrete confined by CFRP jacket should account for the passive nature of confinement in the equations.

6. Conclusion

A constitutive model was represented for confined concrete. Volumetric plastic strain was used as a hardening parameter, and a nonlinear plastic potential was introduced and verified. To model the failure behavior of concrete, fracture energy-based equation were utilized. Crack displacement was considered as a post-peak measure of failure and was imposed onto the yield surface by the decoupled softening function.

The model showed capability of predicting behavior of confined concrete under different levels of confining pressure. The stress-strain curve agreed favorably with the experimental data, especially in the peak and post-peak regions, signifying the robustness of the proposed model.

The behavior of plain concrete confined by a CFRP jacket was studied using passive confinement equations. It was shown that the passive nature of confinement should be included in the constitutive equations to appropriately model the behavior of plain concrete.

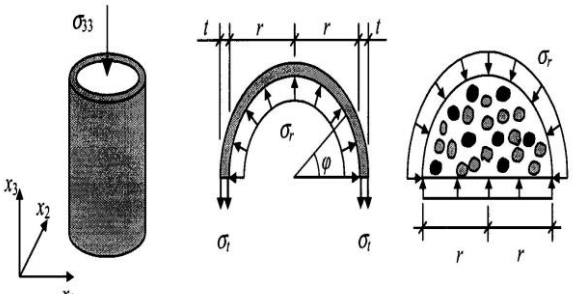

Fig.13: The free body diagram of confined concrete and confining layer [After Grassl et al. 2002 [2]]

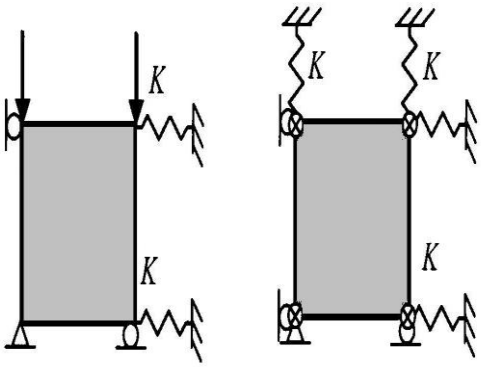

Fig.14: Schematic presentation of considered volume element [After Grassl et al. 2002 [2]]

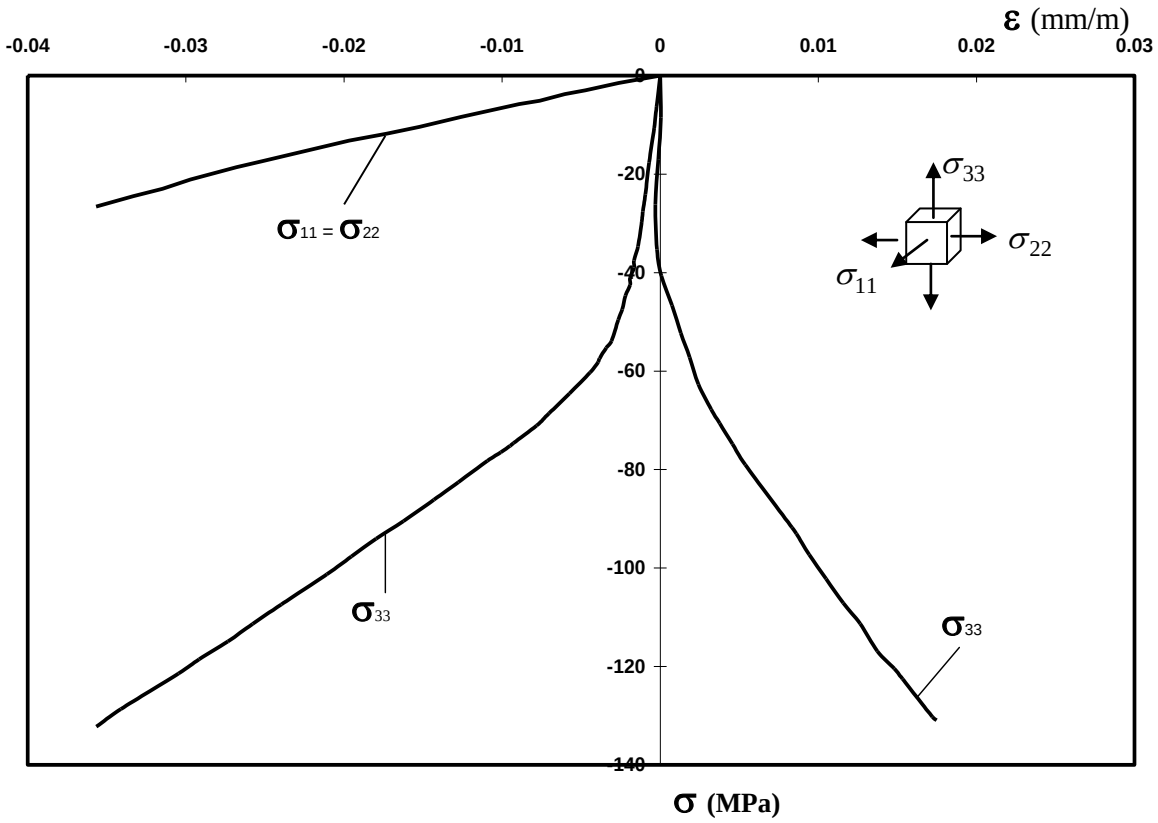

Fig.15: The stress-strain curves in axial and lateral axes for CFRP-confined concrete

References

[1] Imran, I., Pantazopoulou, S.J. (2001), "Plasticity model for concrete under triaxial compression", J. Struct. Eng., ASCE, 126, 281-290.

[2] Grassl P., Lundgren K., Gylltoft K. (2002), "Concrete in compression: a plasticity theory with a novel hardening law", Int. J. Solids Struct., 39, 5205-5223.

[3] Shen, X., Yang, L., Zhu, F. (2004), "A plasticity-based damage model for concrete", Advances in Structural Engineering, 7(5), 461-467.

[4] Spoelstra, M.R., Monti, G. (1999), "FRP-confined concrete model", J. Compos. for Constr., ASCE, 143(3), 143-150.

[5] Mirmiran, A., Shahawy, M. (1997), "Behavior of concrete columns confined by fiber composites", J. Struct. Eng., ASCE, 123(5), 583-590.

[6] Samaan, M., Mirmiran, A., Shahawy, M. (1998), "Model of concrete confined by fiber composites", J. Struct. Eng., ASCE, 124(9), 1025-1031.

[7] Xiao, Y., Wu, H. (2000), "Compressive behavior of concrete confined by carbon fiber composite jackets", J. Materials in Civil Eng., ASCE, 12(2), 139-146.

[8] Menetrey, Ph., Willam, K.J. (1995), "Triaxial failure criterion for concrete and its generalization", ACI Structural Journal, 92 (3), 311-318.

[9] Kupfer, H., Hilsdorf, H.K., Rusch, H. (1969), "Behavior of concrete under biaxial stresses", ACI Journal, title no. 66-52, 656-666.

[10] Van Mier, (1984), "Strain-softening of concrete under multiaxial loading conditions", Eindhoven University of Technology, Eindhoven, The Netherlands, pp. 349.

[11] Imran, I. (1994), "Applications of non-associated plasticity in modelling the mechanical response of concrete", Ph.D. Thesis, Department of Civil Engineering, University of Toronto, Canada, 208pp.

[12] Smith, S.H. (1985), "On fundamental aspects of concrete behavior", M.Sc. Thesis, Department of Civil Engineering, University of Colorado, USA, 192pp.

[13] Bazant, Z.P. (1976), "Inelasticity, ductility and size effect in strain-softening concrete", J. Eng. Mech., ASCE, 102, 331-344.

[14] Hillerborg, A., Modeer, M., and Peterson, P.E. (1976), "Analysis of crack formation and rack growth in concrete by means of fracture mechanics and Finite Element", Cement and concrete Research, 6, 773-782.

[15] Pramono, E., and Willam, K.J. (1989), "Fracture energy-based placticity formulation of plain concrete", J. Eng. Mech., ASCE, 115(6), 1183-1203.

[16] Chen, W.F., Han, D.J. (1988), "Plasticity for Structural Engineers", Springer

[17] Kotsovos, M.D., Newman, J.B. (1980), "Mathematical description of deformational behavior of concrete under generalized stress beyond ultimate strength", J. American Concrete Institute-ACI, 77 (5), 340-346.

[18] Bazant, Z.P., Xiang, Y., Adley, M.D., Prat, P.C., Akers, S.A. (1996), "Microplane model for concrete. II: Data delocalization and verification", J. Eng. Mech., 122 (3), 255-262.